

## Platinum Nanoparticle Catalyst Scavenges Hydrogen Peroxide Generated from Hydroquinone

Kazutaka Hirakawa\* and Shoichiro Sano

Department of Basic Engineering (Chemistry), Faculty of Engineering, Shizuoka University,  
3-5-1 Johoku, Naka-ku, Hamamatsu 432-8561

Received April 9, 2009; E-mail: tkhirak@ipc.shizuoka.ac.jp

Platinum, palladium, gold, rhodium, and silver monometallic nanoparticles protected by poly(*N*-vinyl-2-pyrrolidone), a water-soluble polymer, were prepared using an alcohol reduction method. Platinum/silver bimetallic nanoparticles were prepared by self-organization from the platinum and silver monometallic nanoparticles. Platinum nanoparticles showed the highest catalytic activity for the decomposition of hydrogen peroxide in the monometallic nanoparticles used in this study. Platinum, silver, and platinum/silver nanoparticles effectively catalyzed the decomposition of hydrogen peroxide generated from the autooxidation of hydroquinone, a derivative of carcinogenic benzene. The autooxidation of hydroquinone itself was hardly inhibited by platinum nanoparticles. The platinum nanoparticles in particular showed the highest catalytic activity per unit atom. The activity of a 2 µg platinum nanoparticle was comparable to that of 20 units of catalase. The modification of platinum nanoparticles with silver rather suppressed the activity of hydrogen peroxide decomposition. These results suggest that Pt nanoparticles can be used as antioxidants against oxidative chemical compounds.

The modification of biomacromolecules upon exposure to reactive oxygen species (ROS), including hydrogen peroxide ( $\text{H}_2\text{O}_2$ ), dioxide(1-) (superoxide  $\text{O}_2^{\bullet-}$ ), hydroxyl radical ( $\text{HO}^\bullet$ ), and singlet oxygen ( $^1\text{O}_2$ ), is the likely initial event involved in the induction of the mutagenic and lethal effects of various oxidative stress agents.<sup>1–3</sup> Therefore, the activity of ROS generation by various chemical compounds is closely related to their toxicity, carcinogenicity, or both. For example, hydroquinone, a metabolite of carcinogenic benzene, causes DNA damage via  $\text{H}_2\text{O}_2$  generation.<sup>4</sup> Many studies have addressed the role of antioxidants, such as vitamins<sup>5,6</sup> and catechins,<sup>7</sup> in protection against cancers and cardiovascular diseases. These antioxidants can scavenge ROS and protect against cancer occurrence. On the other hand, every antioxidant is in fact, a redox agent, protecting against ROS in some circumstances and promoting free radical or secondary ROS generation in others. Indeed, an excess of these antioxidants elevates the incidence of cancer.<sup>8,9</sup> Solovieva et al. reported that antioxidants, ascorbic acid<sup>10</sup> and dithiothreitol,<sup>11</sup> exhibit cytotoxicity via  $\text{H}_2\text{O}_2$  generation. Relevantly, it has been reported that vitamins A<sup>12</sup> and E<sup>13</sup> and catechins<sup>14</sup> induce DNA oxidation through  $\text{H}_2\text{O}_2$  generation during their oxidation.  $\text{H}_2\text{O}_2$  is a long-lived ROS which plays an important role in biomacromolecular damage induced by various chemical compounds.<sup>2,4</sup>

Various studies have demonstrated the catalytic decomposition of  $\text{H}_2\text{O}_2$  by noble metals such as platinum (Pt),<sup>15–17</sup> palladium (Pd),<sup>16–18</sup> silver (Ag),<sup>19–21</sup> and gold (Au).<sup>18,21</sup> These metals themselves are hardly oxidized by ROS, however, it is difficult to use metal powder or foils as anti-oxidative drugs. Recently, Kajita et al. reported that Pt nanoparticles catalyze the decomposition of ROS.<sup>22</sup> These nanoparticles can be

dispersed in water and used as homogenous solution. Because this removal mechanism is catalytic decomposition, no oxidized product is formed through this reaction. Platinum metal is used as a food additive and is not considered to be a toxic material. This result led us to the idea that inorganic materials, in particular noble metals, rather than organic antioxidants, can be used as novel chemopreventive agents against ROS-mediated biomolecules damage. In this study, we examined the removal of  $\text{H}_2\text{O}_2$  generated from a chemical compound, hydroquinone, using water-soluble polymer-protected Pt nanoparticles. In addition, the effect of bimetalization<sup>23</sup> of Pt nanoparticles with Ag was investigated. Silver, a relatively inexpensive noble metal, is also used as a food additive.

### Experimental

**Materials.** Dihydrogen hexachloroplatinate(IV) hexahydrate ( $\text{H}_2\text{PtCl}_6 \cdot 6\text{H}_2\text{O}$ ), palladium(II) acetate ( $\text{Pd}(\text{CH}_3\text{COO})_2$ ), rhodium(III) chloride ( $\text{RhCl}_3$ ), hydrogen tetrachloroaurate(III) tetrahydrate ( $\text{HAuCl}_4 \cdot 4\text{H}_2\text{O}$ ), silver nitrate ( $\text{AgNO}_3$ ), sodium tetrahydroborate ( $\text{NaBH}_4$ ), hydroquinone, folic acid, a 30%  $\text{H}_2\text{O}_2$  solution, ethanol, copper(II) chloride, and nicotinamide adenine dinucleotide disodium salt (NADH) were purchased from Wako Pure Chemical Industries (Osaka Japan). Poly(*N*-vinyl-2-pyrrolidone) (PVP, K30, MW: 40000) was from Tokyo Kasei Co. (Tokyo, Japan). Sodium phosphate buffer (pH 7.6) was from Nacalai Tesque Co. (Kyoto, Japan). Catalase (45000 units/mg from bovine liver) was from Sigma Chemical Co. (St. Louis, MO, USA).

Colloidal dispersions of PVP-protected Pt, Pd, Rh, and Au nanoparticles were prepared using an alcohol reduction method.<sup>24</sup> 50 mL of water/ethanol (1/1, v/v) solution containing 1 mM metal salts and 40 mM PVP (monomer unit) was refluxed for 2 h, resulting in the formation of typical colored sols of metal

nanoparticles. The solvent was removed by vacuum evaporation, and the nanoparticles were dispersed into water to prepare 1 mM/atom (atomic concentration) metal colloidal sols. An aqueous solution of PVP-protected Ag nanoparticles<sup>25</sup> was prepared from reduction of 1 mM AgNO<sub>3</sub> with NaBH<sub>4</sub> in the presence of 40 mM PVP. The obtained Ag colloidal dispersion was purified with an ultra-filter. The Ag/Pt (Ag-atom/Pt-atom, 1/1) bimetallic nanoparticles were prepared using a self-organization method to mix Pt and Ag monometallic nanoparticles according to previous reports.<sup>23,26–28</sup>

**Measurements.** The absorption spectra of the colloidal sols were measured with a UV-vis spectrophotometer (UV-1650PC, Shimadzu, Kyoto, Japan). The fluorescence intensity of sample solutions was measured with a fluorescence photometer (650-60, Hitachi, Tokyo, Japan). The absorbance of NADH was measured with an absorbance reader (Sunrise, Tecan Group Ltd., Männedorf, Switzerland). Transmission electron microscopy (TEM), a JEM-2100FX electron microscope (JEOL Ltd., Tokyo, Japan), was used to visualize the metal nanoparticles. Samples for TEM measurement were prepared by placing a drop of colloidal dispersion of metal nanoparticles onto a carbon-coated copper microgrid, followed by naturally evaporating the solvent. The average diameter and standard deviation were calculated by counting the diameters of two handled particles with a magnifier (ten times) on the TEM photograph of 20000 magnification.

**Measurement of the H<sub>2</sub>O<sub>2</sub> Concentration.** The generated H<sub>2</sub>O<sub>2</sub> was measured by a previously reported method using folic acid.<sup>29</sup> This assay is based on the fluorescence enhancement of less-fluorescent folic acid via oxidative decomposition by H<sub>2</sub>O<sub>2</sub> and copper(II) ion into strong-fluorescent 2-amino-4-oxo-3H-pterine-6-carboxylic acid. The concentration of H<sub>2</sub>O<sub>2</sub> ([H<sub>2</sub>O<sub>2</sub>]) can be determined using a calibration curve. A reaction mixture (1 mL) containing 10  $\mu$ M folic acid, 20  $\mu$ M copper(II) chloride, and the H<sub>2</sub>O<sub>2</sub> sample (or H<sub>2</sub>O<sub>2</sub> generator<sup>4</sup>) with or without the metal nanoparticle in a 10 mM sodium phosphate buffer (pH 7.6) was incubated in a microtube (1.5 mL eppendorf) for 30 min. After incubation at 37 °C, the fluorescence intensity of the reaction mixture at 450 nm was measured using a fluorescence photometer with 350-nm excitation.

**Measurement of NADH Consumption.** The consumption of NADH during the autooxidation of hydroquinone was measured by a previously reported method.<sup>4</sup> A sample solution containing 100  $\mu$ M NADH, 50  $\mu$ M hydroquinone, and 20  $\mu$ M copper(II) chloride was incubated at 37 °C in the absence or presence of 20  $\mu$ M/atom Pt nanoparticles. The concentration of NADH was determined by the measurement of absorbance of NADH at 340 nm using a microplate absorbance reader.

## Results

**Preparation of Metal Nanoparticles.** These PVP-protected metal nanoparticles formed water-soluble sols. The average diameters ( $d$ ) and standard deviations ( $\sigma$ ) of monometallic nanoparticles determined by TEM measurement were as follows: Pt ( $d = 2.2$  nm,  $\sigma = 1.0$  nm), Pd ( $d = 2.0$  nm,  $\sigma = 0.9$  nm), Rh ( $d = 2.2$  nm,  $\sigma = 1.0$  nm), Ag ( $d = 10.0$  nm,  $\sigma = 1.9$  nm), and Au ( $d = 10.2$  nm,  $\sigma = 2.0$  nm). The absorption spectrum of the sol of Pt nanoparticles is a flat curve (Figure 1A), indicating the formation of homogenous particles. Ag nanoparticles exhibited a typical yellow color due to surface plasmon absorption around 400 nm. It has been reported that a physical mixture of Ag and Pt nanoparticles

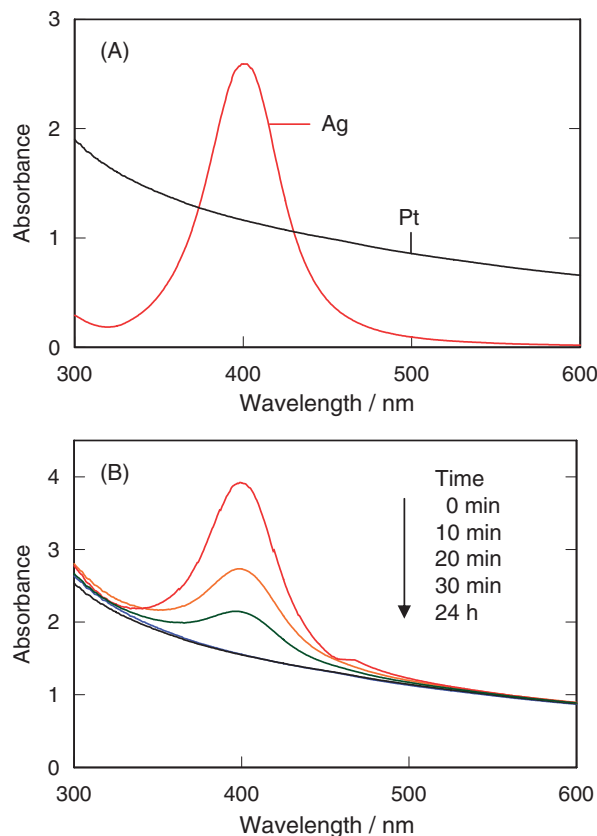


**Figure 1.** Absorption spectra of PVP-protected metal nanoparticle dispersions. The sample solution contained 0.5 mM/atom Ag or Pt nanoparticles in water (A). Absorption spectral change of the physical mixture of dispersions of Ag and Pt nanoparticles (B). The aqueous solutions of Ag (1 mM/atom, 10 mL) and Pt (1 mM/atom, 10 mL) nanoparticles were mixed and measured at 0, 10, 20, and 30 min, and 24 h after mixing.

spontaneously forms bimetallic nanoparticles, possibly Ag-core/Pt-shell structured particles.<sup>26</sup> The time-course of the absorption spectra of this physical mixture showed the extinction of Ag surface plasmon absorption, and the absorption was completely extinguished within 24 h (Figure 1B), suggesting that the surface of the formed bimetallic nanoparticles is composed of Pt atoms. Typical TEM images showed the formation of relatively small particles of Pt and large particles of Ag (Figures 2A and 2B). TEM photographs showed that the large Ag particles disappeared through interaction with Pt particles, resulting in the formation of bimetallic particles smaller than the parent Ag particles (Figure 2C). A similar result has been observed in the case of Ag/Rh bimetallic nanoparticles.<sup>23</sup> These findings suggest the formation of self-organized Ag/Pt bimetallic nanoparticles. These metal nanoparticles are stable in water for several months.

**Catalytic Decomposition of H<sub>2</sub>O<sub>2</sub> by Metal Nanoparticles.** Platinum nanoparticles effectively scavenged H<sub>2</sub>O<sub>2</sub> in a dose-dependent manner and showed the highest activity among the metal nanoparticles used in this study (Figure 3). A sample solution of 5  $\mu$ M/atom Pt nanoparticles, among which 1  $\mu$ g

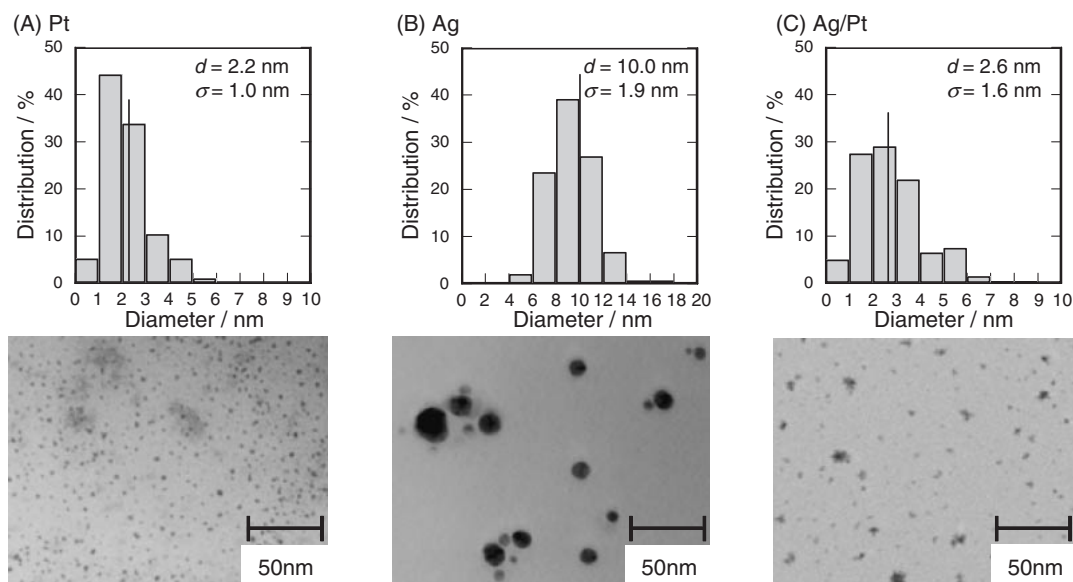


**Figure 2.** Transmission electron micrographs and particle size distribution histograms of metal nanoparticles. The sample of Ag/Pt nanoparticles was prepared by drying the mixtures of the aqueous solutions of Pt and Ag monometallic nanoparticles 24 h after mixing.

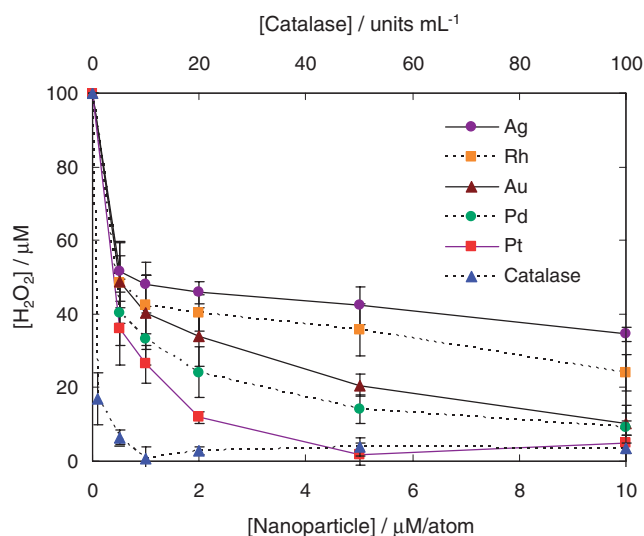
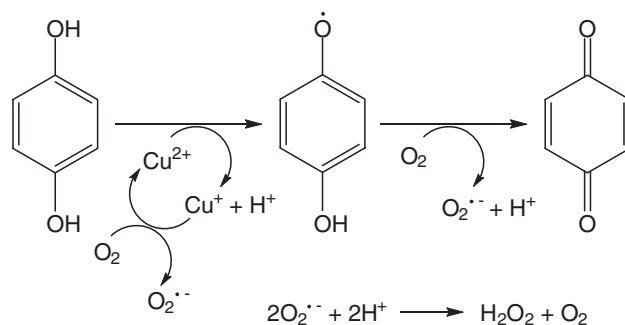
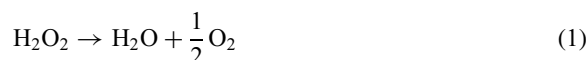


**Figure 3.** Removal of  $\text{H}_2\text{O}_2$  by metal nanoparticles and catalase. The 1 mL of sample solution containing 100  $\mu\text{M}$   $\text{H}_2\text{O}_2$ , 10  $\mu\text{M}$  folic acid, 20  $\mu\text{M}$  copper(II) chloride, and indicated concentration of metal nanoparticles or catalase was incubated for 30 min. The concentration of  $\text{H}_2\text{O}_2$  was estimated from the fluorescence measurement.

Pt metal is included, exhibits comparable activity for  $\text{H}_2\text{O}_2$  decomposition to that of 10 units of catalase. One unit of catalase can remove 1.0  $\mu\text{mol}$   $\text{H}_2\text{O}_2$  per min in water (pH 7.0, 25  $^\circ\text{C}$ ). PVP itself did not scavenge  $\text{H}_2\text{O}_2$  (data not shown). This experiment confirmed that PVP-protected Pt nanoparticles can remove  $\text{H}_2\text{O}_2$ . The mechanism of  $\text{H}_2\text{O}_2$  removal by Pt nanoparticles can be explained by catalytic decomposition into water and molecular oxygen as follows:



**Scheme 1.**

The generation of  $\text{O}_2$  gas through the  $\text{H}_2\text{O}_2$  decomposition was confirmed with a gas-burette.<sup>30</sup>

**Removal of  $\text{H}_2\text{O}_2$  Generated from Hydroquinone by Pt and Ag Nanoparticles.** The catalytic activity of Pt and its modified particles with Ag (Ag/Pt) on the decomposition of  $\text{H}_2\text{O}_2$  generated from chemical compounds was evaluated, since Pt showed the highest activity. Hydroquinone, which is a metabolite of carcinogenic benzene, was used as  $\text{H}_2\text{O}_2$  source. This compound can generate  $\text{H}_2\text{O}_2$  through autooxidation (Scheme 1).<sup>4</sup> Under these experimental conditions, hydroquinone generated  $\text{H}_2\text{O}_2$  in a dose-dependent manner (Figure 4). Twenty units/mL catalase effectively removed  $\text{H}_2\text{O}_2$  generated from this system, and 10  $\mu\text{M}/\text{atom}$  ( $2 \mu\text{g mL}^{-1}$ ) Pt nanoparticles exhibited a comparable activity to that of this catalase. Silver nanoparticles showed apparently weaker activity for  $\text{H}_2\text{O}_2$  removal than Pt nanoparticles. The bimetalization of Pt with Ag apparently suppressed the catalytic activity per unit atom.

Figure 5 shows the removal activity of  $\text{H}_2\text{O}_2$  generated from a high concentration of hydroquinone (50  $\mu\text{M}$ ) by metal nanoparticles. These metal nanoparticles and catalase scavenged  $\text{H}_2\text{O}_2$  in a dose-dependent manner. The activity of the 10  $\mu\text{M}/\text{atom}$  ( $2 \mu\text{g mL}^{-1}$ ) Pt nanoparticles was comparable to

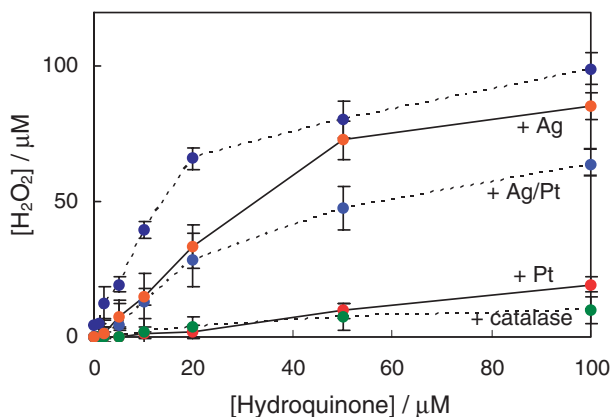


**Figure 4.**  $\text{H}_2\text{O}_2$  generation through autooxidation of hydroquinone in the absence or presence of metal nanoparticles and catalase. The 1 mL of sample solution containing 10  $\mu\text{M}$  folic acid, 20  $\mu\text{M}$  copper(II) chloride, and indicated concentration of hydroquinone with or without 10  $\mu\text{M}$ /atom metal nanoparticles or 20 units/mL catalase was incubated for 30 min. The concentration of generated  $\text{H}_2\text{O}_2$  was estimated from the fluorescence measurement.

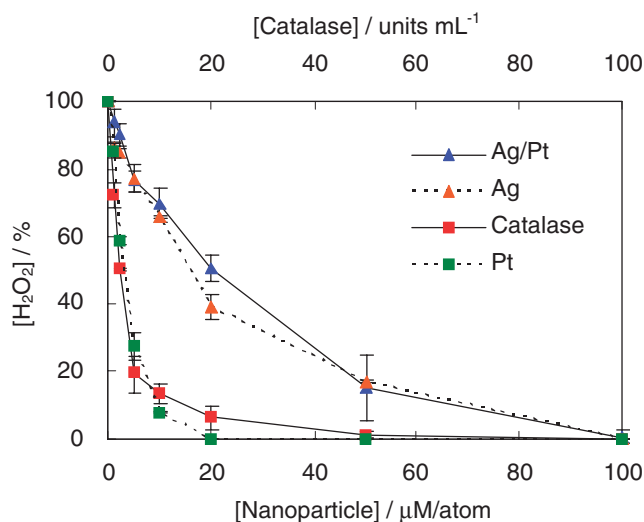


**Figure 5.** Removal of  $\text{H}_2\text{O}_2$  generated through the autooxidation of hydroquinone by metal nanoparticles and catalase. The 1 mL of sample solution containing 10  $\mu\text{M}$  folic acid, 20  $\mu\text{M}$  copper(II) chloride, 50  $\mu\text{M}$  hydroquinone, and indicated concentration of metal nanoparticles or catalase was incubated for 30 min. The concentration of  $\text{H}_2\text{O}_2$  was estimated from the fluorescence measurement.

that of 20 units/mL catalase, and Pt completely scavenged  $\text{H}_2\text{O}_2$  over 20  $\mu\text{M}$ /atom ( $4 \mu\text{g mL}^{-1}$ ). The activity per atom of the Ag/Pt bimetallic nanoparticles was almost the same as that of the Ag monometallic nanoparticles.

**Effect of Pt Nanoparticles on the Autooxidation of Hydroquinone.** To investigate the effect of Pt nanoparticles on  $\text{H}_2\text{O}_2$  generation through the autooxidation of hydroquinone, NADH consumption during this autooxidation was measured. The oxidized form of hydroquinone can be reduced into the parent hydroquinone by NADH.<sup>4</sup> The concentration of NADH was gradually decreased through the redox of hydro-

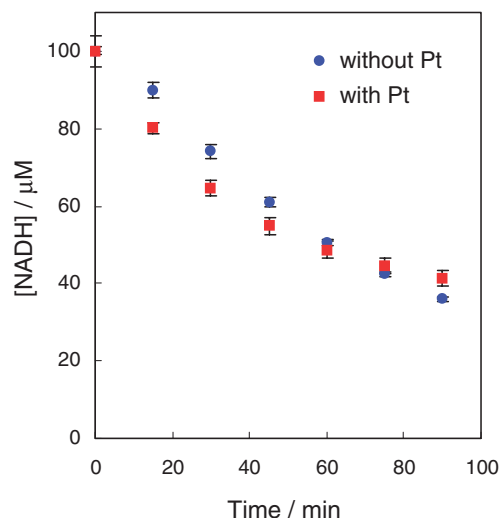


**Figure 6.** NADH consumption through the autooxidation of hydroquinone in the absence or presence of Pt nanoparticle. The sample solution containing 100  $\mu\text{M}$  NADH, 50  $\mu\text{M}$  hydroquinone, 20  $\mu\text{M}$  copper(II) chloride, and 20  $\mu\text{M}$ /atom Pt nanoparticle was incubated. The concentration of NADH was monitored by absorption measurement at 340 nm.

quinone and Pt nanoparticles hardly inhibited NADH consumption (Figure 6). This result indicated that Pt nanoparticles do not inhibit the  $\text{H}_2\text{O}_2$  generation itself, because  $\text{H}_2\text{O}_2$  is produced through the autooxidation of hydroquinone.

### Discussion

PVP-protected metal nanoparticles, in particular Pt nanoparticles, exhibited a removal effect on  $\text{H}_2\text{O}_2$  generated through autooxidation of hydroquinone. The  $\text{H}_2\text{O}_2$  generation was hardly inhibited by Pt nanoparticles. The removal of  $\text{H}_2\text{O}_2$  by these metal nanoparticles can be explained by a catalytic reaction similar to that by catalase, which decomposes  $\text{H}_2\text{O}_2$  into  $\text{H}_2\text{O}$  and  $\text{O}_2$ . The formation of  $\text{H}_2\text{O}_2$  during autooxidation of hydroquinone is through  $\text{O}_2^{\bullet-}$ , which is generated from a reduction of  $\text{O}_2$  by hydroquinone.<sup>4</sup> Because the lifetime of  $\text{O}_2^{\bullet-}$ , which dismutates into  $\text{H}_2\text{O}_2$  through reaction with  $\text{H}^+$ , is short (ca. 0.1 ms), the scavenging of  $\text{O}_2^{\bullet-}$  by a metal nanoparticle can be negligible.<sup>31</sup> The  $\text{H}_2\text{O}_2$  removal activity per metal atom of these metal nanoparticles occurred in the following order: Pt > Ag  $\approx$  Ag/Pt. The activities of  $\text{H}_2\text{O}_2$  decomposition per metal atom consisting of these metal nanoparticles ( $\mu\text{M-H}_2\text{O}_2/\mu\text{M-nanometal}$ ) have been estimated from the slope of the initial plots in Figure 5, and the resulting values are 4.2, 12.2, and 3.8 for Ag, Pt, and Ag/Pt, respectively. Further, the activity on the surface area of the Ag/Pt nanoparticles ( $17 \mu\text{M-H}_2\text{O}_2/\text{cm}^2\text{-nanometal}$ )<sup>32</sup> was also smaller than that of Pt ( $49 \mu\text{M-H}_2\text{O}_2/\text{cm}^2\text{-nanometal}$ ). These findings showed that the Pt nanoparticles have the highest catalytic activity for  $\text{H}_2\text{O}_2$  decomposition of the metal nanoparticles used in this experiment and the activity of Pt nanoparticles is suppressed by modification with Ag.

$\text{H}_2\text{O}_2$  is a long-lived ROS and plays an important role in DNA damage.<sup>2,4</sup> Indeed, various chemical compounds, including carcinogens, generate  $\text{H}_2\text{O}_2$  during redox.<sup>2,4</sup> Molecular

oxygen is easily reduced by various compounds, leading to the formation of  $\text{O}_2^{\bullet-}$ . Formed  $\text{O}_2^{\bullet-}$  is rapidly dismutated into  $\text{H}_2\text{O}_2$ . Although  $\text{H}_2\text{O}_2$  itself is not a strong reactive species, it can generate highly reactive  $\text{HO}^\bullet$  through a Fenton reaction or a Haber–Weiss reaction. Furthermore,  $\text{H}_2\text{O}_2$  can penetrate a cytoplasm membrane and be incorporated into the cell nucleus. Therefore,  $\text{H}_2\text{O}_2$  is considered to be one of the most important reactive species or a precursor participating in carcinogenesis. The removal of  $\text{H}_2\text{O}_2$  is an effective method for cancer chemoprevention. Furthermore, protective agents against  $\text{H}_2\text{O}_2$  are important to treat acatalasemia, a genetic deficiency of erythrocyte catalase inherited as an autosomal recessive trait. Antioxidants, such as vitamins A and E, are effective protective agents. However, the oxidized products of antioxidants or these molecules themselves promote the formation of secondary  $\text{H}_2\text{O}_2$ .<sup>12,13</sup> Indeed, an excess of these antioxidants elevates the incidence of cancer.<sup>8,9</sup> A catalyst consisting of an inorganic stable material is not oxidized and does not generate secondary ROS. Water-soluble nanoparticles of noble metal may become novel protective agents against ROS.

### Conclusion

Pt, Ag, and Ag/Pt nanoparticles effectively scavenge  $\text{H}_2\text{O}_2$  generated from autooxidation of a highly concentrated hydroquinone. Platinum nanoparticles exhibited the highest catalytic activity among these nanoparticles. Pt is a very stable metal against various chemical compounds and permitted as a food additives. The noble metal nanoparticles may be used as novel chemopreventive agents for cancer or other non-malignant conditions induced by chemical compounds through  $\text{H}_2\text{O}_2$  generation.

The authors wish to thank Professor Kenji Murakami (Research Institute of Electronics, Shizuoka University) for his helpful advice on TEM measurement. This work was supported by a Grant-in-Aid for Scientific Research from the Ministry of Education, Culture, Sports, Science and Technology (MEXT) of the Japanese Government.

### References

- 1 J. Cadet, T. Douki, D. Gasparutto, J.-L. Ravanat, *Mutat. Res., Fundam. Mol. Mech. Mutagen.* **2003**, 531, 5.
- 2 S. Kawanishi, Y. Hiraku, S. Oikawa, *Mutat. Res., Fundam. Mol. Mech. Mutagen.* **2001**, 488, 65.
- 3 D. A. Drechsel, M. Patel, *Free Radical Biol. Med.* **2008**, 44, 1873.
- 4 K. Hirakawa, S. Oikawa, Y. Hiraku, I. Hirokawa, S. Kawanishi, *Chem. Res. Toxicol.* **2002**, 15, 76.
- 5 T. J. Slaga, *Crit. Rev. Food Sci. Nutr.* **1995**, 35, 51.
- 6 M. Sohmiya, M. Tanaka, K. Okamoto, A. Fujisawa, Y. Yamamoto, *Neurol. Res.* **2004**, 26, 418.
- 7 M. J. Weyant, A. M. Carothers, A. J. Dannenberg, M. M. Bertagnolli, *Cancer Res.* **2001**, 61, 118.
- 8 Y. Nitta, K. Kamiya, M. Tanimoto, S. Sadamoto, O. Niwa, K. Yokoro, *Jpn. J. Cancer Res.* **1991**, 82, 511.
- 9 G. S. Omenn, G. E. Goodman, M. D. Thornquist, J. Balmes, M. R. Cullen, A. Glass, J. P. Keogh, F. L. Meyskens, Jr., B. Valanis, J. H. Williams, Jr., S. Barnhart, M. G. Cherniack, C. A. Brodtkin, S. Hammar, *J. Natl. Cancer Inst.* **1996**, 88, 1550.
- 10 M. E. Solovieva, V. V. Soloviev, V. S. Akatov, *Eur. J. Pharmacol.* **2007**, 566, 206.
- 11 M. E. Solovieva, V. V. Soloviev, A. A. Kudryavtsev, Y. A. Trizna, V. S. Akatov, *Free Radical Biol. Med.* **2008**, 44, 1846.
- 12 M. Murata, S. Kawanishi, *J. Biol. Chem.* **2000**, 275, 2003.
- 13 N. Yamashita, M. Murata, S. Inoue, M. J. Burkitt, L. Milne, S. Kawanishi, *Chem. Res. Toxicol.* **1998**, 11, 855.
- 14 S. Oikawa, A. Furukawa, H. Asada, K. Hirakawa, S. Kawanishi, *Free Radical Res.* **2003**, 37, 881.
- 15 K. B. Keating, A. G. Rozner, J. L. Youngblood, *J. Catal.* **1965**, 4, 608.
- 16 D. W. McKee, *J. Catal.* **1969**, 14, 355.
- 17 G. Bianchi, F. Mazza, T. Mussini, *Electrochim. Acta* **1962**, 7, 457.
- 18 D. D. Eley, D. M. Macmahon, *J. Colloid Interface Sci.* **1972**, 38, 502.
- 19 K. Goszner, D. Körner, R. Hite, *J. Catal.* **1972**, 25, 245.
- 20 H. J. Baumgartner, G. C. Hood, J. M. Monger, R. M. Roberts, C. E. Sanborn, *J. Catal.* **1963**, 2, 405.
- 21 K. Goszner, H. Bischof, *J. Catal.* **1974**, 32, 175.
- 22 M. Kajita, K. Hikosaka, M. Iitsuka, A. Kanayama, N. Toshima, Y. Miyamoto, *Free Radical Res.* **2007**, 41, 615.
- 23 K. Hirakawa, N. Toshima, *Chem. Lett.* **2003**, 32, 78.
- 24 H. Hirai, Y. Nakao, N. Toshima, *J. Macromol. Sci., Part A: Pure Appl. Chem.* **1979**, 13, 727.
- 25 Y. Shiraishi, N. Toshima, *J. Mol. Catal. A: Chem.* **1999**, 141, 187.
- 26 N. Toshima, M. Kanemaru, Y. Shiraishi, Y. Koga, *J. Phys. Chem. B* **2005**, 109, 16326.
- 27 N. Toshima, Y. Shiraishi, T. Matsushita, H. Mukai, K. Hirakawa, *Int. J. Nanosci.* **2002**, 1, 397.
- 28 T. Matsushita, Y. Shiraishi, S. Horiuchi, N. Toshima, *Bull. Chem. Soc. Jpn.* **2007**, 80, 1217.
- 29 K. Hirakawa, *Anal. Bioanal. Chem.* **2006**, 386, 244.
- 30 The 10 mL of aqueous solution containing 0.1 M  $\text{H}_2\text{O}_2$  was treated by 10  $\mu\text{g}$  Pt nanoparticles and generated  $\text{O}_2$  gas was measured with a gas-burette. The volume of detected gas coincided with that of the theoretically calculated value of  $\text{O}_2$  generation from the decomposition of  $\text{H}_2\text{O}_2$  in the sample solution.
- 31 Under these experimental conditions, one Pt nanoparticle (average diameter: 2.2 nm) consists of about 370 Pt atoms, indicating that the sample solution of 10  $\mu\text{M}$ /atom Pt contains 0.027  $\mu\text{M}$  Pt nanoparticles. The diffusion control limit of the collision rate ( $\text{s}^{-1}$ ) in aqueous solution is expressed by  $7 \times 10^9 \times [\text{Particle concentration}]$ , and the reciprocal of this value indicates that the effective reaction between  $\text{O}_2^{\bullet-}$  and one nanoparticle requires more than 5 ms. Because the lifetime of  $\text{O}_2^{\bullet-}$  is about 1 ms, the decomposition of  $\text{O}_2^{\bullet-}$  by Pt nanoparticles may be negligible.
- 32 The total surface area ( $S$ ) of nanoparticles in sample solution can be expressed as follows:  $S = 6cVA_w/\rho d$  where  $c$ ,  $V$ ,  $A_w$ , and  $\rho$  are atomic concentration of nanoparticles, volume of sample solution (1 mL), atomic weight of metal (Ag: 107.87 g mol<sup>-1</sup>, Pt: 195.08 g mol<sup>-1</sup>, Ag/Pt: average of those of Ag and Pt, 151.48 g mol<sup>-1</sup>), and density of metal (Ag: 10.49 g cm<sup>-3</sup>, Pt: 21.45 g cm<sup>-3</sup>, Ag/Pt: average of those of Ag and Pt, 15.97 g cm<sup>-3</sup>), respectively. When  $V$  is 1  $\mu\text{M}$ , the  $S$  value indicates the total surface area of 1  $\mu\text{M}$ /atom nanoparticles. The activities on the surface area of metal nanoparticles are computable to divide the slopes of Figure 5 by these  $S$  values.